DEVELOPMENT OF SUSTAINABLE CEMENTLESS MORTARS

Keun-Hyeok Yang[1], Seol Lee[2], and Sang-Ho Nam[3]

[1] Assistant Professor, Department of Architectural Engineering, Mokpo National University, South Korea
[2] Ph.D. Student, Department of Architectural Engineering, Mokpo National University, South Korea
[3] Associate Professor, Department of Chemistry, Mokpo National University, South Korea
Correspond to yangkh@mokpo.ac.kr

ABSTRACT: Nine alkali-activated (AA) mortars were mixed and cured at water or air-dried conditions to explore the significance and limitation for the application of the combination of Ba and Ca ions as an alkali-activator. Ground granulated blast-furnace slag (GGBS) was used for source materials, and calcium hydroxide ($Ca(OH)_2$) and barium hydroxide ($Ba(OH)_2$) were employed as alkali activators. Test results clearly showed that the water curing condition was more effective than the air-dried curing condition for the formation of the denser calcium silicate hydrate (C-S-H) gels that had a higher molar Si/Ca ratio, resulting in a higher strength development. At the same time, the introduction of $Ba(OH)_2$ led to the formation of $2CaO \cdot Al_2O_3 \cdot SiO_2 \cdot 8H_2O$ (C_2ASH_8) hydrates with higher molar Si/Al and Ca/Al ratios. Based on the test results, it can be concluded that the developed cementless mortars have highly effective performance and high potential as an eco-friendly sustainable building material.

Keywords: alkali-activated mortar; compressive strength; hydration products; eco-friendly material

1. INTRODUCTION

The reduction of greenhouse gas (GHS) emissions is one of the hottest issues all over the world. The Kyoto Protocol has aimed for a 5.2% lower emission amount of GHS between 2008 and 2012 compared with that in 1990. It is generally estimated that the amount of GHS emitted from the worldwide production of ordinary Portland cement (OPC) corresponds to approximately 7% of the total GHS emissions into the Earth's atmosphere [1]. In addition, serious environmental problems have also encountered from the production of OPC [2], such as environmental pollution by dust and enormous energy consumption from plasticity temperature being over 1300℃. A large proportion of the concrete industry is very interested in reducing GHS emissions. With the extensive effort to minimize carbon dioxide emissions, alkali-activated ground granulated blast-furnace slag (GGBS) binder has been investigated in many fields [3-4] to produce cementless mortar or concrete. As a result, it has been generally recognized [4] that GGBS-based alkali-activated (AA) binders are practically useful construction materials owing to their sound environmental performance such as recycling of by-product materials, low carbon dioxide emissions and low energy consumption. In addition, AA concrete has been known to have many beneficial properties compared with ordinary Portland cement (OPC) concrete such as rapid high strength development, good durability and high

resistance to chemical attack [3]. As a result, the application of AA mortar or concrete has gradually grown to a large proportion in the construction industry.

In the present study, 9 AA mortars were mixed and tested to develop the cementless mortars activated by a powder typed barium hydroxide ($Ba(OH)_2$) and calcium hydroxide ($Ca(OH)_2$). The flow loss and compressive strength development against the elapse of time were recorded in the fresh and hardened mortars, respectively. The hydration products and microstructural characteristics of the AA pastes sampled from the AA mortars tested were also traced using X-ray diffraction (XRD) and energy-dispersive X-ray (EDX) analyses combined with a scanning electron microscope (SEM) image. The compressive strength development and hydration products of the mixed AA mortars were compared according to the curing condition.

2. EXPERIMENTAL DETAILS

2.1 Materials and mix proportions

Ground granulated blast-furnace slag (GGBS), which is commercially available worldwide, was activated by a powder typed barium hydroxide ($Ba(OH)_2$) and calcium hydroxide ($Ca(OH)_2$). The $Ca(OH)_2$-to-GGBS ratio by weight were 0% and 7.5%, and the $Ba(OH)_2$-to-GGBS ratio by weight varied from 0 to 10% at a spacing of 2.5%. The chemical compositions of the GGBS evaluated by x-ray fluorescence (XRF) analysis are given in Table 1. The molar ratios of the major element in the GGBS

determined by EDX analysis are given in Table 2. The GGBS used for the source material had a high CaO content and SiO_2-to-Al_2O_3 ratio by mass of 2.29. The molar silica-to-alumina, calcium-to-alumina and silica-to-calcium ratios of the used GGBS are approximately 2.3, 4.52, and 0.51, respectively. The measured specific gravity and specific surface area of GGBS were 2.9 and 4400 cm^2/g, respectively. The maximum particle sizes of $Ca(OH)_2$ and $Ba(OH)_2$ were 21.2 μm, and 26.7 μm, respectively. Locally available sand was used as fine aggregate in a saturated surface dry condition. The specific gravity, grading and maximum size of sand particles used were 2.54, 2.97 and 5mm, respectively.

2.2 Casting, curing, and testing

The GGBS, alkali activators and fine aggregate were dry-mixed in a mixer pan for 1 minute, and water was then added and mixed in for another 1 minute. After testing for the initial flow, each mix was poured into 50 mm steel cube moulds in order to evaluate the compressive strength of the mortar specimens. o examine the effect of curing circumstances on the compressive strength development and hydration products of the mixed AA mortars, both air-dried curing at room temperature and water curing at 21°C conditions were used. Immediately after casting, all specimens were cured individually at room temperature and all steel moulds were removed at an age of one day. After removing steel moulds, half of the hardened mortars for each mix were cured at the water condition and the others were cured at

Table 1. Chemical composition of GGBS used (% by mass).

Materials	SiO_2	Al_2O_3	Fe_2O_3	CaO	MgO	TiO_2	LOI[*]
GGBS	35.5	12.6	0.6	40.3	9.0	0.7	0.8

* Loss on ignition.

Table 2. Molar ratios of the major elements of GGBS used.

Si/Al	Ca/Al	Si/Ca	Mg/Al	Mg/Ca	Mg/Si
2.25	2.93	0.77	0.31	0.10	0.14

the air-dried condition until they were tested at an age schemed to measure the compressive strength and hydration products of the mixed AA mortars.

The flow of different mortars was recorded at 0 (initial), 30, 60, 90 and 120 minutes after mixing in order to examine the flow loss against the elapse of time. The compressive strengths of the mortars were measured at 1, 3, 7, 28, 56 and 91 days using a 200 kN capacity Universal Testing Machine (UTM) in order to investigate the gain in strength with age. The test procedures were carried out according to the specifications of the Korean Industrial Standard [5] for testing OPC mortar, KS L 5111 for flow and KS L 5105 for compressive strength. To evaluate the effect of $Ba(OH)_2$ and the curing condition on the hydration products and reactivity mechanism of the mixed AA mortars, XRD and EDX analyses combined with an SEM image were carried out on specimens C7.5B0 and C7.5B5 at the age of 1, 3, 7, 28 and 91 days.

3. TEST RESULTS AND DISCUSSION

3.1 Materials and mix proportions

The initial flow of the tested AA mortar increased with the increase of R_B, up to R_B =7.5%, beyond which it decreased slightly, as given in Table 3. When R_B was at the same level, the initial flow decreased with the increase of R_C. Although GGBS is classified not into pozzolans but into cementitious materials [6], the reactivity between GGBS, $Ca(OH)_2$ and water is very similar to that of the lime-pozzolan reaction [7]. The reactivity of pozzolan is influenced by the specific surface area and soluble fraction of $Ca(OH)_2$ [4]. Therefore, a higher $Ca(OH)_2$ content can result in a poor workability in $Ca(OH)_2$-activated GGBS mortars due to a higher dissolution of $Ca(OH)_2$.

On the other hand, the flow loss of the tested AA mortar against the elapsed time was also significantly influenced by R_C, but was almost independent on R_B, as shown in Fig. 1. The flow of $Ba(OH)_2$-activated GGBS mortars decreased with the elapse of time up to 60

Table 3. Summary of test results

| Specimen[*]	R_C (%)	R_B (%)	F (mm)					$f_c^{'}$ (MPa)										
								Air-dried curing						Water curing				
			Initial	30 mins	60 mins	90 mins	120 mins	1 day	3 days	7 days	28 days	56 days	91 days	3 days	7 days	28 days	56 days	91 days
C0B2.5	0	2.5	149	123	116	115	112	3.0	5.4	7.5	7.6	8.0	8.1	4.0	8.9	18.3	21.9	24.8
C0B5		5.0	151	127	119	117	117	2.7	5.4	7.1	7.1	6.8	7.4	4.3	8.5	14.0	16.2	17.6
C0B7.5		7.5	163	148	136	136	135	2.5	6.9	8.7	8.2	8.4	8.1	6.3	9.8	15.7	16.4	18.5
C0B10		10.0	159	143	137	136	134	2.6	7.0	9.8	10.5	12.2	11.3	6.9	12.2	18.4	22.2	23.8
C7.5B0	7.5	0	123	105	102	100	100	2.9	9.4	10.5	13.8	10.7	9.5	9.6	15.7	21.7	22.7	22.5
C7.5B2.5		2.5	136	121	116	112	110	6.7	14.6	15.9	19.8	25.5	26.7	12.4	21.0	28.1	31.9	32.5
C7.5B5		5.0	141	127	122	120	117	3.6	11.3	13.1	15.0	16.2	18.3	10.2	16.2	24.9	26.1	26.9
C7.5B7.5		7.5	144	135	129	125	120	3.5	11.3	14.4	15.3	16.6	17.7	11.1	17.1	23.8	26.2	26.6
C7.5B10		10.0	136	135	130	125	121	3.4	11.4	14.4	15.1	16.2	18.4	10.8	16.2	22.6	26.2	26.4

Note: F and $f_c^{'}$ indicate flow and compressive strength of mortars tested, respectively.
* The mortar specimen notation includes four identifiers for the selected parameters. The first and third parts represent the type of alkali activator added: C for $Ca(OH)_2$ and B for $Ba(OH)_2$. The second and fourth parts are used to identify the $Ca(OH)_2$-to-GGBS ratio, R_C, and the $Ba(OH)_2$-to-GGBS ratio, R_B, respectively.

minutes, beyond which it remained nearly constant. On the other hand, the flows for Ca(OH)$_2$ and Ba(OH)$_2$-activated GGBS mortars decreased almost linearly, regardless of R_B, showing that the decreasing rate was more prominent with the increase of R_C. The flow of the Ca(OH)$_2$-activated GGBS mortar specimen C7.5B0 was not developed after 90 minutes, indicating that they entered hardening. However, the flow of Ca(OH)$_2$ and Ba(OH)$_2$-activated GGBS mortars maintained above 80% of their initial flow even after 120 minutes, indicating that the addition of Ba(OH)$_2$ can contribute to the retardation of the setting time of AA mortars. The initial flow and flow loss of GGBS-based mortars activated only by the Ca(OH)$_2$ were relatively mean, but were significantly superior to those of the GGBS-based mortars that were activated by sodium silicate or sodium hydroxide. Therefore, the development of the enhanced workability and delayed setting time of AA mortars by using Ca(OH)$_2$ and Ba(OH)$_2$ would be useful in order for them to become widely applicable construction materials.

3.2 Compressive strength at 28 days

The effect of the used alkali activators on the compressive strength at the age of 28 days f_c' of AA mortars cured at different conditions is presented in Fig. 2.
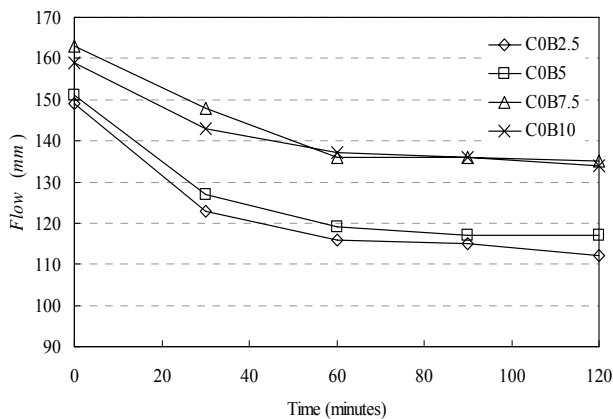
(a) R_C=0%
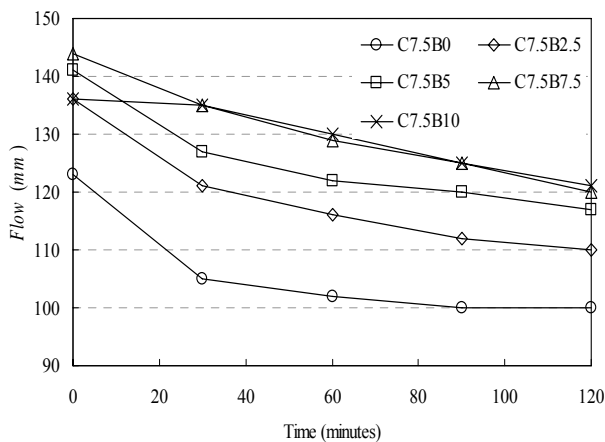
(b) R_C=7.5%

Fig 1. Flow variation against the elapsed time.

The curing condition had a significant influence on the f_c' of the tested AA mortars. For the same level of R_B, the f_c' of the AA mortars cured at water was higher than that of the AA mortars cured at air drying by an average of 201% and 151% for R_C=0% and 7.5%, respectively, showing that the difference of f_c' against the curing condition decreased with the increase of R_C. The effect of the addition of Ba(OH)$_2$ on f_c' of the AA mortars was more significant in water curing than in air-dried curing. In addition, the ratio f_c' of water-cured AA mortar to that of air-cured AA mortar slightly increased with the increase of R_B up to R_B=5%, with the exception of specimen C0B2.5, beyond which it decreased. The f_c' of mortar activated only by the Ba(OH)$_2$ increased slightly with the increase of R_B when R_B was above 5%, regardless of the curing condition. Conversely, when R_C was 7.5%, the f_c' of Ca(OH)$_2$ and Ba(OH)$_2$-activated GGBS mortars increased up to R_B=2.5%, beyond which it slightly decreased. This observed trend was independent of the curing condition.

3.3 Compressive strength development

The compressive strength developments against the age of different AA mortars cured at air drying and at water are shown in Fig. 3 and Fig. 4, respectively. The 1-day compressive strengths of air-cured AA mortars were approximately 30% and 22% of its 28-day compressive strength, for R_C=0% and 7.5%, respectively. The compressive strength development of Ca(OH)$_2$ and Ba(OH)$_2$-activated GGBS mortars at an early age was independent of the amount of Ba(OH)$_2$ added. This means that the reaction rate between GGBS and Ca(OH)$_2$ or Ba(OH)$_2$ slows noticeably. On the other hand, the compressive strength of air-cured AA mortars after 7 days was significantly affected by the amount of Ba(OH)$_2$ added. The compressive strength of the air-cured mortars activated only by the Ba(OH)$_2$ was almost remained constant after 7 days, regardless of R_B, as shown in Fig. 3 (a).
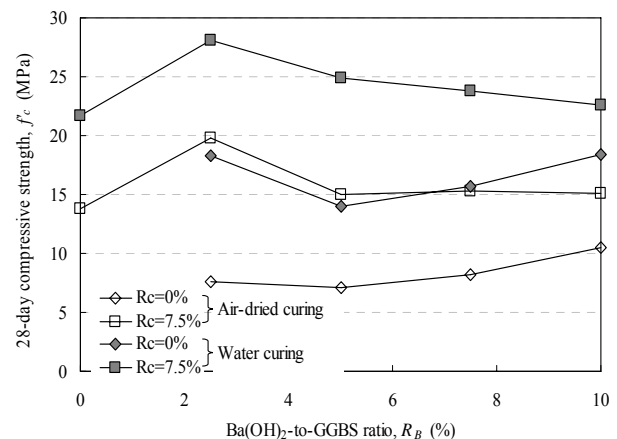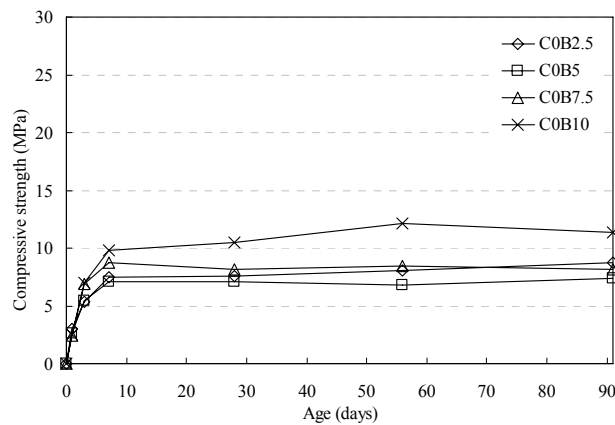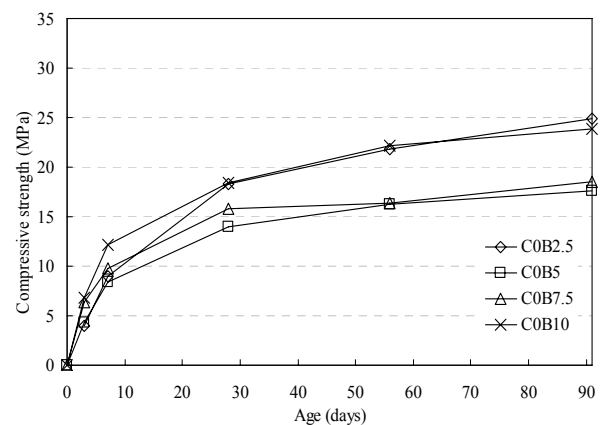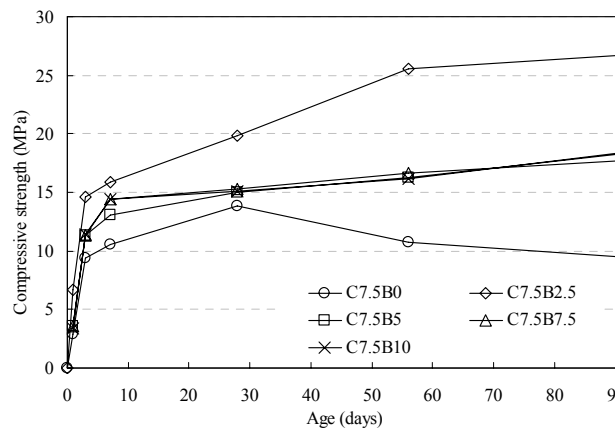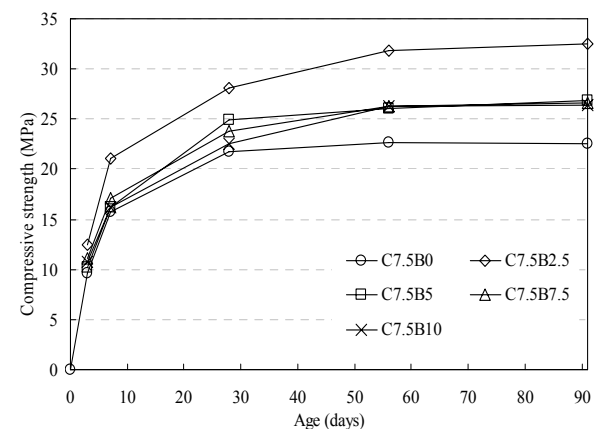

Fig 2. Compressive strength of AA mortars at 28 days.

For the air-cured AA mortars with R_C =7.5%, the compressive strength at age of 7 days was ranged between 75% and 95% of 28-day strength, showing that 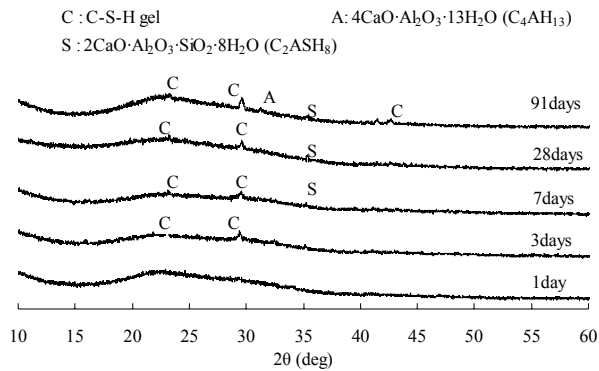the strength gain rate increased with the increase of R_B. The compressive strength gain of air-cured AA mortars after 28 days was also influenced by the amount of Ba(OH)$_2$ added. The compressive strength of air-cured mortars activated only by the Ca(OH)$_2$ reduced after 56 days by an average of 15% of their own 28-day strength, whereas that of AA mortars in which Ba(OH)$_2$ was added improved significantly at a long-term age. As reported by Shi et al. [4], Ca(OH)$_2$ in the Ca(OH)$_2$-activated GGBS pastes is depleted rapidly for the first 3 days, and the reaction rate of Ca(OH)$_2$ significantly decreased after 14 days, which causes an unstable strength development at a long-term age. The addition of less than 2.5% Ba(OH)$_2$ can stabilize the reactivity of Ca(OH)$_2$-activated GGBS pastes at a long-term age, and results in improving their long-term strength.

The characteristics of strength development of water-cured AA mortars are generally similar to those of air-cured AA mortars. This can be represented by a parabolic curve. However, a higher strength was commonly developed in water-cured AA mortars than in air-cured AA mortars at both the early and long-term ages.

Moreover, the ratio of strength gain to the 28-day strength of water-cured AA mortars compared with that of the company air-cured AA mortars was higher at a long-term age, though it was lower at an early age.

3.4 XRD analysis

The XRD patterns of pastes sampled from specimens C7.5B0 and C7.5B5 measured at different ages are shown in Fig. 5 and Fig. 6, respectively. For the air-cured AA mortars, no distinct diffraction peaks could be observed on the XRD patterns of both specimens up to 1 day, while calcium silicate hydrate (C-S-H) gel then appeared as a main hydration product after 3 days. For specimen C7.5B0 cured at air drying, 2CaO·Al$_2$O$_3$·SiO$_2$·8H$_2$O (C$_2$ASH$_8$) and 4CaO·Al$_2$O$_3$·13H$_2$O (C$_4$AH$_{13}$) were also observed as hydration products after 7 days and at 91 days, respectively, but their diffraction peaks were very weak. Water-cured C7.5B0 also showed 2MgO·SiO$_2$·xH$_2$O (M$_2$SH$_x$) after 7 days, and the diffraction peaks for C-S-H gel, C$_2$ASH$_8$ and C$_4$AH$_{13}$ were more intensified compared with those of the company specimen cured at air drying. These trends were also observed for specimen C7.5B5. This indicates that water curing contributes to the acceleration of the reactivity between GGBS and the used activators. As a result, a higher strength can be developed as shown in Figs. 3 and 4. For specimen

(a) R_C=0%

(b) R_C=7.5%

Fig 3. Compressive strength development against age of AA mortars cured at air drying.

(a) R_C=0%

(b) R_C=7.5%

Fig 4. Compressive strength development against age of AA mortars cured at water.

C : C-S-H gel   A: 4CaO·Al₂O₃·13H₂O (C₄AH₁₃)
S : 2CaO·Al₂O₃·SiO₂·8H₂O (C₂ASH₈)

(a) Air dry curing

C : C-S-H gel   A: 4CaO·Al₂O₃·13H₂O (C₄AH₁₃)
S : 2CaO·Al₂O₃·SiO₂·8H₂O (C₂ASH₈) M: 2MgO·SiO₂·xH₂O (M₂SHx)
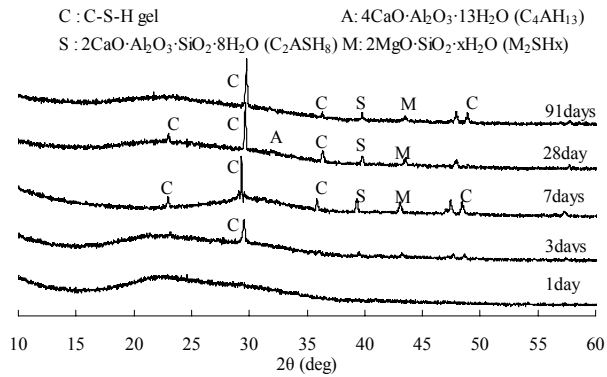
(b) Water curing

Fig 5. XRD patterns of Ca(OH)₂-activated GGBS pastes sampled from C7.5B0.

C : C-S-H gel   A: 4CaO·Al₂O₃·13H₂O (C₄AH₁₃)
S : 2CaO·Al₂O₃·SiO₂·8H₂O (C₂ASH₈) M: 2MgO·SiO₂·xH₂O (M₂SHx)

(a) Air dry curing

C : C-S-H gel   A: 4CaO·Al₂O₃·13H₂O (C₄AH₁₃)
S : 2CaO·Al₂O₃·SiO₂·8H₂O (C₂ASH₈) M: 2MgO·SiO₂·xH₂O (M₂SHx)
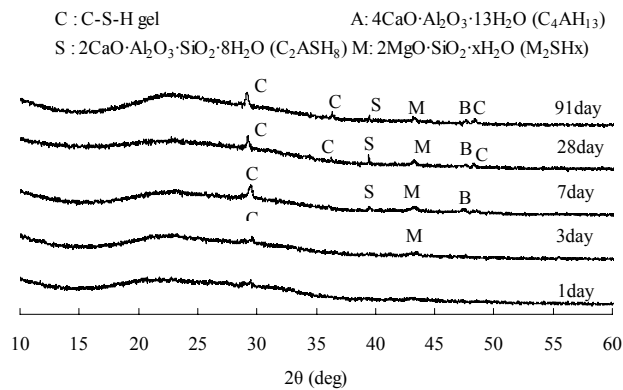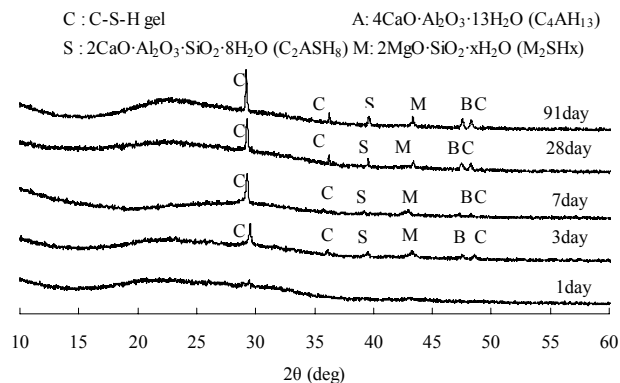
(b) Water curing

Fig 6. XRD patterns of Ca(OH)₂ and Ba(OH)₂-activated GGBS pastes sampled from C7.5B5.

C7.5B5, barite (BaSO₄) was also detected as a main hydration product after 3 days, in addition to the hydration products observed in specimen C7.5B0, while C₂ASH₈ appeared after 1 day. This may be attributed to the addition of Ba(OH)₂. In particular, higher diffraction peaks and wider diffuse bands for the hydration products were developed in specimen C7.5B5 than in specimen C7.5B0, which could lead to a higher compressive strength gain of the mortars. Wang et al. [7] showed that C-S-H gel tightly sorbing sodium cations, C₂ASH₈, and C₄AH₁₃ can be developed as main hydration products for the GGBS mortars activated by sodium silicate or sodium hydroxide. Figures 5 and 6 clearly show that Ca(OH)₂ and Ba(OH)₂-activated GGBS mortars generated M₂SHₓ and BaSO₄ in addition to C-S-H gel, C₂ASH₈, and C₄AH₁₃. As the age proceeded, the diffuse peaks for the hydration products gradually intensified, showing that the intensities were more notable in water-cured AA mortars than in air-cured AA mortars, and in specimen C7.5B5 than in C7.5B0. This indicates that the addition of Ba(OH)₂ and water curing can have a significant effect on the intensities of hydration products.

3.5 SEM/EDX analyses

Figure 7 shows SEM images of pastes sampled from specimen C7.5B0. The main molar ratios obtained from EDX analyses for the different morphology of hydration products are also given in these figures. At the age of 1 day, large irregular hexagonal plates covered by partially hydrated crust products were observed. The molar Si/Ca ratio of the hexagonal plates was 0.58 for Ca(OH)₂-activated GGBS mortars, of which values were lower compared with that of GGBS used as a source material as given in Table 2. This may be attributed to the addition of Ca(OH)₂. On the other hand, the molar Si/Al ratio of the hexagonal plates was similar to that of GGBS. Therefore, considering the microstructural morphology of GGBS, the hexagonal plates would be estimated to be the fractional phases of GGBS prior to reactivity with the alkali-activator. At 3 days, no hexagonal plates were found, yet a number of crust hydration products were still observed in air-cured specimen C7.5B0. In addition, the microstructure of water-cured AA mortars was denser than that of air-cured AA mortars. After 7 days, the C-S-H gels were radiantly developed. The growth of hydration products was more prominent in the water curing condition than in the air-dried condition. The mircrostructures of the specimens at 28 days were very similar to those at 7 days. At 91 days, a slight difference appeared in the structure of the tested AA mortars. The structure of specimen C7.5B0 cured at air drying became looser, while that of water cured-mortar specimen was denser and coagulated products became stabilized.

The most detectable hydration product was C-S-H gel in all tested AA mortars as shown in the XRD patterns. Therefore, the hydration products that were found easily in the SEM images would be estimated to be C-S-H gels formed around slag particles. The molar Si/Ca ratio in the C-S-H gels generally increased with the increase of hydration time. In addition, a higher molar Si/Ca ratio
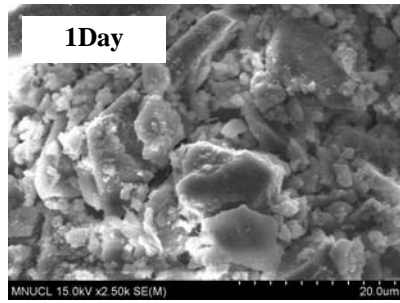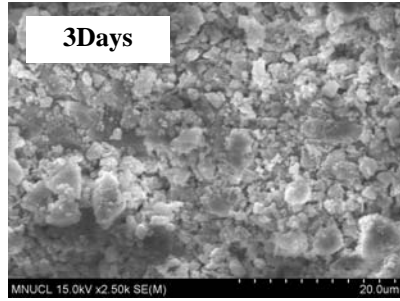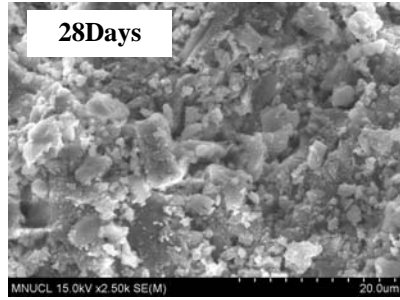
was developed in water-cured AA mortars than in air-cured AA mortars. In particular, the molar Si/Ca ratio of specimen C7.5B0 cured at air drying dropped at the age of 91 days. From the comparison with strength results represented in Fig. 2, it can be suggested that the C-S-H gel that has a higher molar Si/Ca ratio is favorable for enhancing the compressive strength of GGBS-based AA mortars, though the exact mechanism is not known yet.
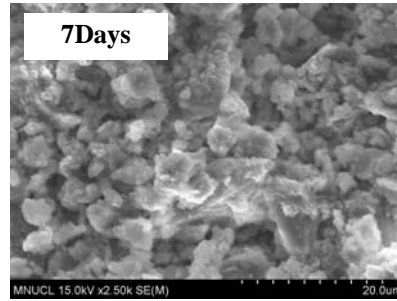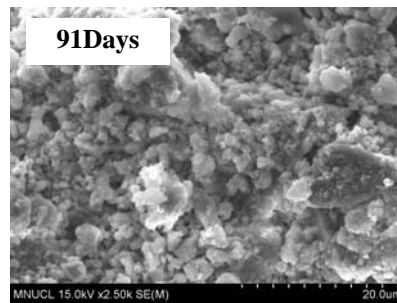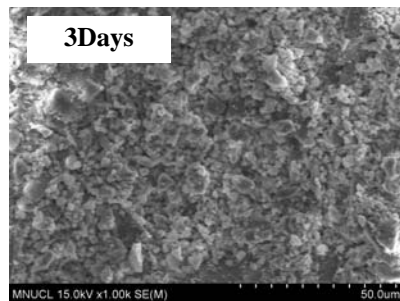

(a) Air dry curing
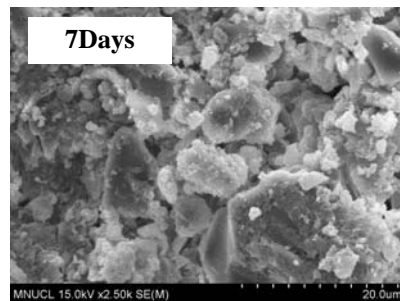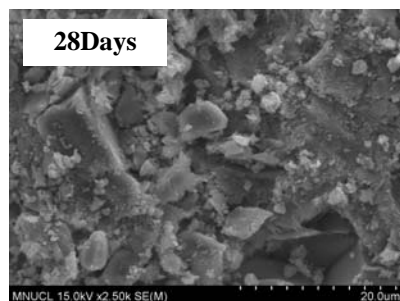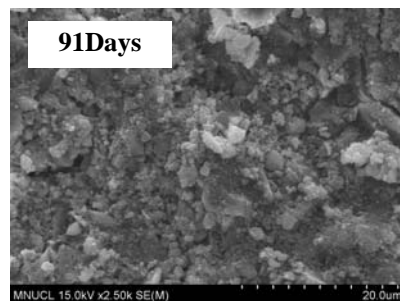
(b) Water curing

Fig. 7-SEM images of Ca(OH)$_2$-activated GGBS pastes sampled from C7.5B0.

4. CONCLUSIONS

Nine alkali-activated (AA) ground granulated blast-furnace slag (GGBS) mortars were mixed and cured at air-dried or water conditions. The $Ca(OH)_2$-to-GGBS ratio, R_C, by weight were 0% and 7.5%, and the $Ba(OH)_2$-to-GGBS ratio, R_B, by weight varied from 0 to 10% at a spacing of 2.5%.

1. The initial flow of AA mortar increased with the increase of R_B and with the decrease of R_C. In particular, $Ba(OH)_2$ can contribute to the retardation of the setting time of AA mortars.

2. The compressive strength of AA mortars cured at water was higher than that of AA mortars cured at air drying, showing that the difference of strength against the curing condition decreased with the increase of R_C.

3. The compressive strength of mortars activated only by the $Ba(OH)_2$ increased slightly with the increase of R_B, whereas that of $Ca(OH)_2$ and $Ba(OH)_2$-activated GGBS mortars increased up to R_B=2.5%, beyond which it slightly decreased, regardless of the curing condition.

4. The compressive strength development of $Ca(OH)_2$ and $Ba(OH)_2$-activated GGBS mortars was independent of the addition amount of $Ba(OH)_2$ at an early age. On the other hand, the compressive strength gain rate of the air-cured AA mortars with R_C =7.5% at an early age increased with the increase of R_B.

5. The observed hydration products of $Ca(OH)_2$-activated GGBS mortars were calcium silicate hydrate (C-S-H) gel, $2CaO·Al_2O_3·SiO_2·8H_2O$ (C_2ASH_8), $4CaO·Al_2O_3·13H_2O$ (C4AH13), and $2MgO·3SiO_2·XH_2O$ ($M_2S_3H_x$), while barite ($BaSO_4$) also appeared in addition to these hydrates for $Ca(OH)_2$ and $Ba(OH)_2$-activated GGBS mortars.

6. For the air-cured AA mortars, no distinct diffraction peaks could be observed on the XRD patterns up to 1 day.

The diffuse peaks for the hydration products gradually intensified as the age proceeded, indicating that the intensities were more notable in water-cured AA mortars than in air-cured AA mortars, and in $Ca(OH)_2$-activated GGBS mortars than in $Ca(OH)_2$ and $Ba(OH)_2$-activated GGBS mortars.

REFERENCES

[1] Malhotra VM, Mehta PK. "Pozzolanic and cementitious materials.", *Gordon and Breach Publishers*, . USA.1996.
[2] Yang KH, Song JK, Ashour AF, Lee ET. "Properties of cementless mortar activated by sodium silicate.", *Construction and Building Materials*. Vol. 22(8), pp. 1981-1989, 2008.
[3] Wang SD, Pu XC, Scrivener KL, Pratt PL. "Alkali-activated slag cement and concrete: a review of properties and problems.", *Advances in Cement Research*, Vol. 27, pp. 93-102, 1995.
[4] Shi C, Krivenko PV, Roy D. "Alkali-activated cements and concretes.", *Taylor and Francis*; 2006.
[5] Korean Standards Information Center. "Korean industrial standard.", South Korea, 2006.
[6] ASTM C 618. "Standard specification for coal fly ash and raw or calcined natural pozzolan for use as a mineral admixture in concrete.", *Annual Book of ASTM Standards. American Society for Testing & Materials*. Philadelphia, USA, 2003.
[7] Wang SD, Scrivener KL, Pratt PL. "Factors affecting the strength of alkali-activated slag." *Cement and Concrete Research*., Vol. 24(6), pp. 1033-1043, 1994.